Originally published in *Proceedings of the Fifth International Workshop on Compressible Turbulent Mixing*, ed. R. Young, J. Glimm & B. Boston.
ISBN 9810229100, World Scientific (1996).

Shock-Induced Instability Experiments on Gas Interfaces Featuring a Single Discrete Perturbation

N. Cowperthwaite, M. Philpott, A. V. Smith,
A. D. Smith, and D. Youngs

AWE Aldermaston
Reading RG7 4PR
ENGLAND

Abstract. This paper describes the experimental investigation using laser sheet interrogation of the Richtmyer-Meshkov shock-induced instability growth of a single discrete perturbation imposed on an otherwise plane membrane separating two gases of different density. Two perturbations, both of 2D geometry are examined; a rectangular notch facing upstream and a shallow circular bump facing downstream, both using fine wire meshes to support and profile the membranes. For comparison, experiments have also been performed with a plane membrane with no additional perturbation.
Direct 3D numerical simulation using the TURMOIL3D code is used to perform calculations with the discrete perturbation (notch or bump) plus a random perturbation to initiate the growth of the 1D turbulent mixing zone. Good agreement is obtained with the experimental results.

1 Introduction

This study followed as an extension to the investigations reported by Landeg et al. (1993) at the 4$^{\text{th}}$ IWCTM. In common with the earlier work, the test series reported here was conducted at shock Mach No. 1.26 (shock pressure 10 psi, 69 kPa) using the AWE (Foulness) 20 $\times$ 5 cm shock-tube with a 3-zone arrangement of air/freon-12/air (Figure 1). As before, gas separation was by microfilm membranes, cast from Micro-X solution as a double layer of thickness typically not exceeding 1 micron. Visualization of the gas mixing process was by means of pulsed laser sheet illumination of the seeded freon-12 gas, with a synchronized rotating drum camera (Figure 2) recording up to 100 high quality 35 mm film images per experiment. This multi-frame arrangement has

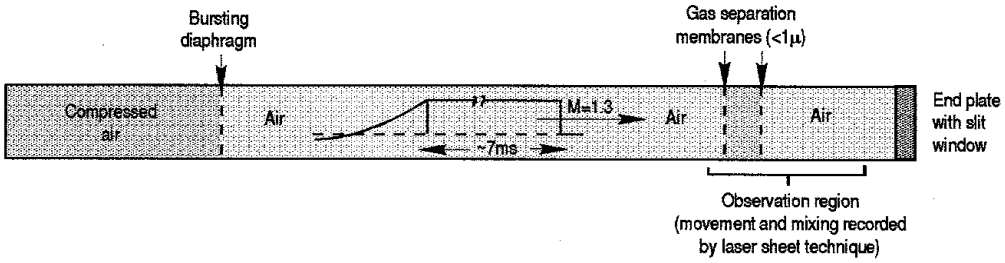

Figure 1: 20 × 5cm shock tube.

shown significant advantages over single-shot systems such as that reported by Meshkov et al. at the 2nd IWCTM for use on similar experiments.

The previous work investigated both plane and sinusoidally perturbed gas interfaces (Figure 3a) with attention focused on the observed mixing development across both upstream and downstream interfaces resulting from passage of the incident and subsequent reflected shocks. Following advances made in the technique for profiling the micro-film membranes used to separate the gases (described under 'Use of wire meshes'), the current test series as reported here deviated from the earlier series by featuring a small single perturbation at the downstream boundary. The small size is emphasized by including an example of an 'actual size' notch in Figure 3b showing its size of 7mm × 7mm in relation to the shock tube dimensions.

2 Aim of Tests

These latest experiments served two purposes. With reference to Figure 4, showing some of the perturbations investigated,

1. They show the effect of a small isolated perturbation superimposed on a flat[1] membrane on the growth of the turbulent mixing zone.

2. In conjunction with the 3D numerical simulation, they provide results for validating 2D turbulence models.

A comparison between experimental data and 3D results will be illustrated.

[1]The 2D turbulence model calculation includes representation of the perturbation imposed on the 'flat' membrane caused by the wire mesh support (i.e. initial wavelength is of the order of the mesh spacing). An initial random perturbation of similar amplitude and wavelength is also used in the 3D simulations. Relevant data are included later under 'TURMOIL3D Code Calculations'.

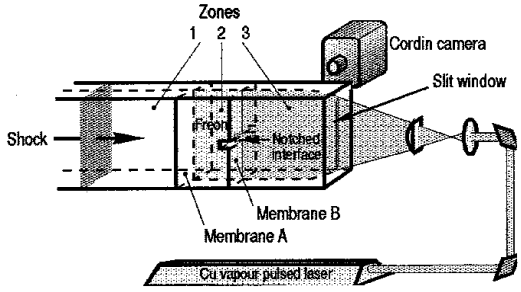

Figure 2: Laser sheet set-up.

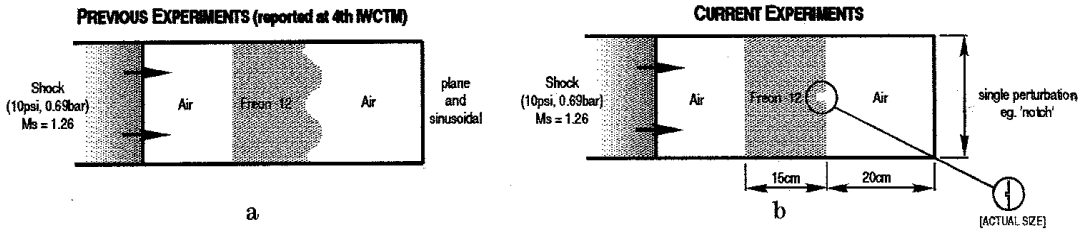

Figure 3: Sinusoidal and single discrete perturbations investigated at down stream boundary.

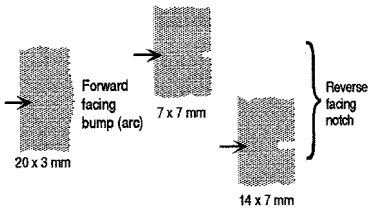

Figure 4: Perturbation profiles investigated.

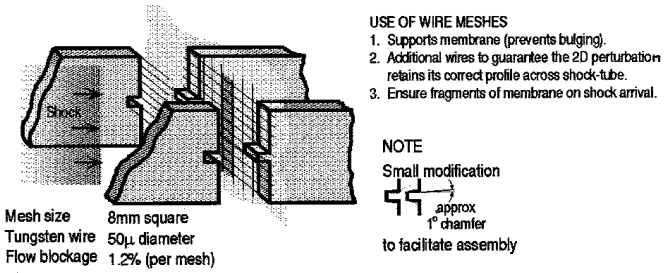

Figure 5: Use of wire meshes as membrane support.

3 Profiles Investigated

The profiles of the perturbations reported are shown in Figure 4. They consist of the square and rectangular notch (recessed), and the forward facing bump (protruding). Dimensions are as shown, sized to define approximately equal masses of added or lost freon gas respectively contained by the bump and 7 mm square notch perturbation. This 'defect' mass represents 0.17% of the total freon gas mass. An extension to the notch test series is currently in progress investigating the reverse-facing configuration converted to forward-facing. The dotted outline of the mesh wires supporting the membrane is for reference only.

4 Use of Wire Meshes to Support and Profile Membranes

Figure 5 illustrates the use of wire meshes formed from fine wire of 50 micron diameter and 8 mm square aperture to support the membranes. They were used in pairs to sandwich the membrane at both the air/freon and freon/air boundaries. They serve three function; to ensure fragmentation of the membrane on shock arrival, to prevent pre-shock membrane from bulging, and to define (using additional wires) the required 2D perturbation profile. A necessary modification to facilitate assembly of the test section is indicated in Figure 5.

Flow blockage was 1.2% per mesh. Meshes generally remained intact after a test, though not reusable.

5 Laser Sheet Imaging Details

Laser:

Cu-vapor (Oxford Lasers type 15A).

Frequency, 511 and 578 nm; Operating Speed, typically 20,000 pulses per second.

Pulse Duration, 30 ns; Pulse Energy, 2 mJ per pulse; Sheet Thickness, 1-2 mm (in test section).

Camera:

Cordin 35 mm drum camera (synchronized to pulsed laser via Oxford Lasers 'N' shot controller); 100 frames over 5 ms (typical).

Seeding:

(principal scattering process is Mie Scattering)

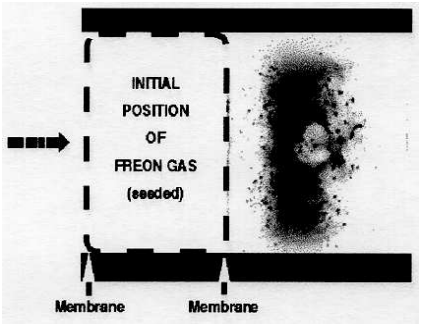

Figure 6: Sample unprocessed image.

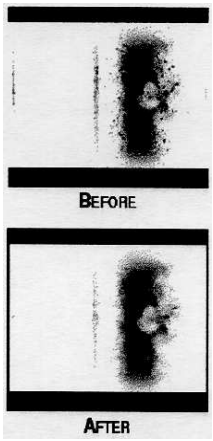

Figure 7: Fragment removal.

Olive Oil; aerosol generated in compressed freon-12 within TSI atomizer (model 9302A); Droplet Size, water/air, in range 0.2-3 micron diameter (TSI data), olive oil/freon, - same range assumed (unconfirmed); Increase in freon density, $\sim 1\%$.

Image Digitization:

Camera, CCD; JVC, resolution 768×512 pixels; Grey Scale; 0-255 values; Global Lab Image software.

6 Interpretation of Sample Image

[All photographic results are reproduced as digitized images.]

The sample unprocessed image shown in Figure 6 is extracted from a Cordin camera sequence of seventy 35 mm film negatives recording a 'bump' perturbation experiment. The full-view pre-shock position of the freon zone (20 cm high$\times$15 cm long) is clearly marked, while 20 cm downstream, less clearly visible, is a faint line near to the right hand extremity representing the face of the transparent end-plate.

With shock front arrival (from the left of the figure) at the first membrane defined as time zero, the frame shown corresponds to about 2 ms. By this time the incident shock front (shock duration, 7 ms, flat-top) has traversed and compressed the gases in the test section, reached the end plate, and reflected back through itself at enhanced pressure to

progress back upstream through the developing mix region. Several secondary reflected and rarefaction waves have also been generated at the gas interfaces.

Visually, the image reveals a compressed freon zone, still intact at 2 ms, with its boundaries becoming mixed with the air on either side. The central initially small perturbation has undergone a phase inversion and developed into a gross structure. Numerous fragments from both membranes are clearly visible confirming successful break-up. From this single laser sheet image, certain problems of analysis can be appreciated.

7 Problems in Laser Sheet Image Analysis

Several problems arose in image analysis, exemplified by the following.

A significant problem, that of fragment removal, has been effectively solved by applying an algorithm to each digitized image. A prototype has produced the 'before' and 'after' results shown in Figure 7. It involves identifying a suspect fragment, by appropriate analysis of the density gradients of the grey-scale pixel values, and by substituting data representative of the immediate locality. Such processing, partially automated and still under development, is currently applied to around 70 images per experiment.

A further problem relates to the non-uniform spatial intensity of the laser sheet. Despite the laser beam featuring the ideal characteristic of a 'top hat' spatial distribution as opposed to Gaussian, the beam could not be adequately expanded with the optics available to ensure acceptable uniformity over the whole 20 cm height of the test section. Consequently in certain tests, analysis necessarily omitted the outer regions of the images.

Another problem, that of considerable attenuation of light intensity on passage through the unshocked freon, as experienced in earlier tests, was overcome by reducing the seeding concentration.

The major problem concerns uncertainty over the non-linearity of the stages involved in the recording (film) and analysis (via CCD camera) processes. Sufficient data are available to quantify the processes involved; however, incorporation into an analysis package awaits experimental confirmation of an overall calibrated transfer characteristic, preferably coinciding with the proposed implementation of densitometry techniques, proven on radiographic analysis. An alternative interim self-calibrating solution, not fully progressed, involves referencing image intensity in regions of 100% freon at three known pressure levels (pre-shock, post-shock, post-reflected shock). In this paper, analysis is based on linear relationships.

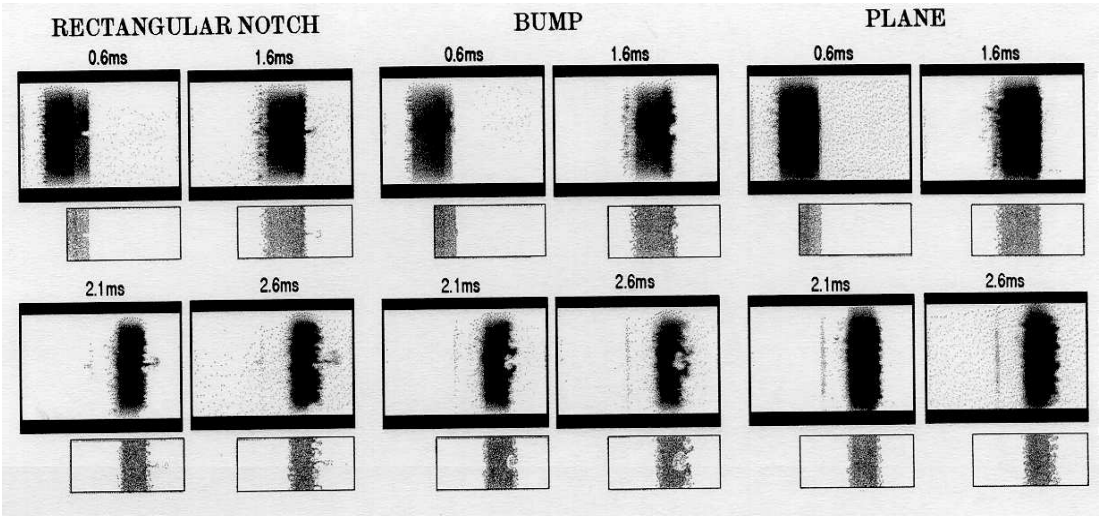

Figure 8: Laser sheet images; above; 2D code, below.

8 Representative Examples of Laser Sheet Images

A sample of digitized laser sheet images (in negative form) is presented in Figure 8, for three of the perturbations studied; bump, rectangular notch, and plane. [NB. For interest, though not discussed until later, is inclusion under each experimental image, of the code result, limited to the half-height (10 cm) central region.]

From the seventy or more images recorded per experiment, four are shown for each perturbation, at approximate times 0.6, 1.6, 2.1, 2.6 ms, relative to shock arrival at the first membrane (time zero). Maximum deviation from these times is half of the frame separation time of 0.067 ms. Common features are described as follows.

0.6 ms: Shows shock compression of the freon gas (as enhanced illumination) behind the shock front as it approaches the undisturbed downstream interface. The perturbation on the latter (i.e. the bump or the notch) is visible near the center line. Obscuring marks are due to traces of sealant remaining on the optical surfaces. Sufficient evidence is seen to exist upstream of the effect of approximately 25 transverse wires (i.e. 8 mm grid spacing over 203 mm height). Light intensity striations within the body of the freon gas are also apparent, due to light reflectance or obscuration by the downstream membrane fragments within the laser sheet.

1.6 ms: Shows, by the further enhanced illumination of the freon, the travel of the reflected shock into the freon en route back upstream. The notch or bump perturbation, inverted in phase during passage of the incident shock, is seen to have undergone

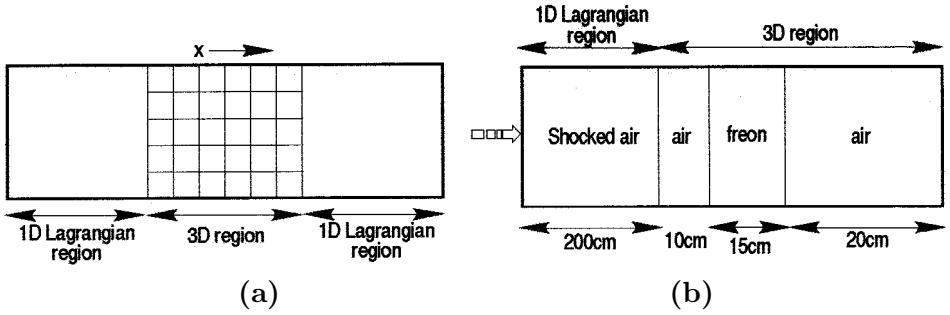

Figure 9: (a) Moving mesh option, (b) test representation.

significant expansion. The 25 node perturbation originating from the upstream mesh accounts for the predominant disturbance across the gas boundaries.

2.1 ms: Following the passage of the reflected shock though the freon zone, the latter is now compressed to about 1/3 of its original volume. Memory of the wire mesh wavelength has largely disappeared along the downstream boundary by selective growth or regrouping into longer wavelength, larger amplitude structures. Upstream, a reduced thickness of mixing zone is apparent due to the combined effects of gas compression and phase inversion, during the reflected shock, of the boundary structures so far developed.

2.6 ms: Further development continues of the central feature and growth of the restructured downstream boundary.

9 TURMOIL3D Code Calculation

Details of the calculations, performed on a Cray YMP computer, are as follows.

Figure 9a shows the moving mesh option as used for shock tube problems, in which the x-direction mesh moves with the mean x-velocity.

If this moving mesh option is used, then 1D Lagrangian regions may be added at the $x_{\min}$ and $x_{\max}$ boundaries, with 3D simulation only performed near the turbulent mixing zone.

Figure 9b shows a representation of the shock tube experiment. The zoning used in the 3D region is $360 \times 160 \times 80$ zones (3D calculations), $360 \times 160 \times 1$ zones (2D calculations).

The initial perturbation imposed on the downstream interface is the defined notch or bump with the superimposition on both interfaces of a random perturbation, representing the effect of membrane fragmentation, of wavelength 0.5 to 5 cm, and amplitude standard deviation 0.01 cm. Similar data applied to the 2D version of the code.

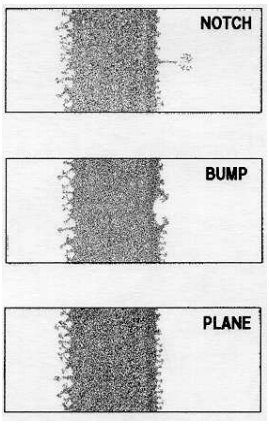

Figure 10: 2D code results at 1.6 ms.

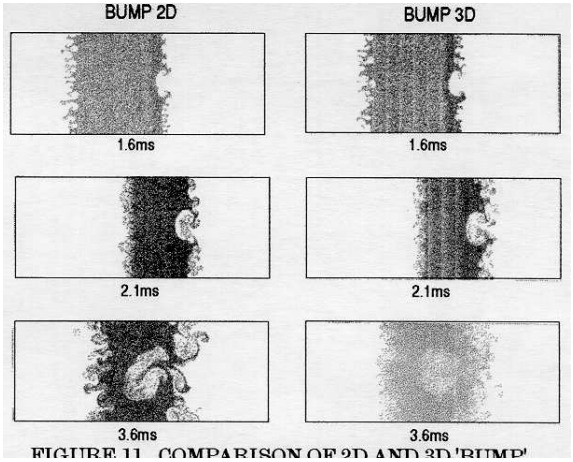

Figure 11: Comparison of 2D and 3D 'bump' results at 3.6 ms. The 3D code reveals fine scale mixing.

Output from the 3D code calculations is typically displayed in the form of mix (freon concentration) contours at 0.05, 0.25, 0.75, 0.95 values at time increments of 0.1 ms increasing to 0.2 ms. Since such concentration data do not reveal the location or presence of shocks and compressed gas states, an alternative display is for freon gas density to be plotted, with print density (i.e. dot concentration) linearly related to gas density, as in Figures 10 and 11. Either can be produced on hard copy, to display gas states as they exist within the central plane, as applicable to the laser sheet, or as a path integral mean in the z (line of viewing) direction.

10 Sample Code Results

10.1 2D Results

Code results showing freon density were included in Figure 8 as small scale plots for comparison with the experimental images: shock progression and other features were described. Repeated in larger display for the same three cases (rectangular notch, bump, plane) at the time 1.6 ms, Figure 10 reveals distinct similarities in mix development. Upstream, the development from the initial small scale perturbation applied to represent the mesh is identical in all three cases. Downstream, a similar situation is apparent, modified by the tendency of those mushroom-type structures close to the central development (whether void or jet) to be drawn along the interface toward, and subsequently into, the central region of activity.

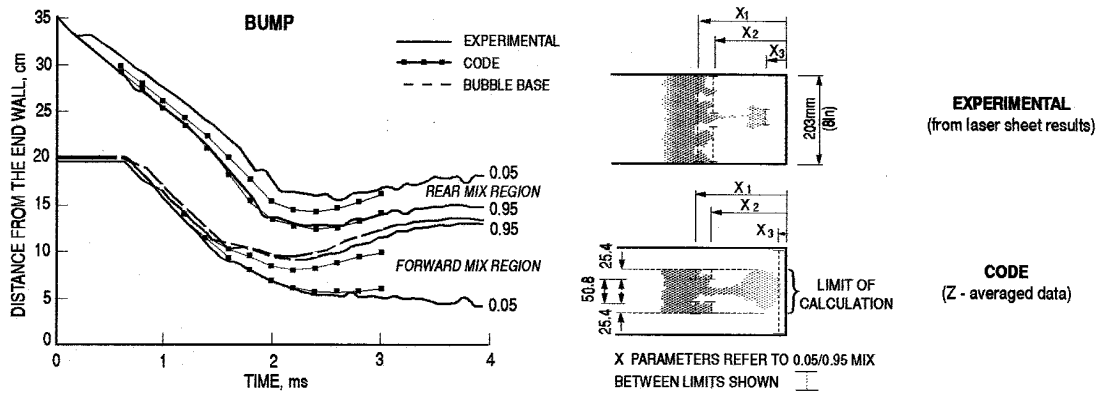

Figure 12: Time/history of freon/air interface (experimental and code).

10.2 3D Results

Figure 11 shows a comparison of 2D vs. 3D density calculations for the bump perturbation case. The 2D result is as in Figure 10 with a 3.6 ms result included. The 3D results, shown for matching times, represent a plane section through the calculation, for direct comparison with the laser sheet images.

While at earlier times little distinction between 2D and 3D results is evident, by 3.6 ms the 3D result shows a markedly different turbulent mix pattern. The well-defined features of the 2D result can be seen to have degraded into fine-scale mixing in the 3D case, more comparable to experimental observations. No significant difference is detected in the 0.05 and 0.95 freon/air concentration limits.

11 Measured Mix Parameters

The measured mix parameters of main interest are as shown in Figure 12, for the notch case. The experimental measurements X_1, X_2 represent the location of the 0.05 and 0.95 (freon/air concentration) mix limits at the downstream boundary, taken as a mean over the full height of the test section, but excluding (for the X_2 measurement) the central region which contains the stalk-like structure (notch tests) or air cavity (bump tests). The X_2 measurement refers to the 0.05 position at the jet head or cavity base. The corresponding code measurements, based on 0.05/0.95 limits, are similarly determined though between different limits as shown.

12 Comparison of Code and Experimental Results

Applying the above measurement criteria to the experimental and code results typified by Figure 8 provides distance-time histories such as shown in Figure 12. This shows, for a bump experiment and corresponding 2D calculation, the positional movement of the 0.05 and 0.95 mix limits at both the upstream and downstream boundaries. Also tracked are key features describing the growth of the central structure originating from the initial perturbation, in this case, the cavity extremity. Code comparison shows respectable agreement on displacement of the air/freon boundaries, though with an under-prediction of mix widths.

Regarding this latter discrepancy, further attention must be paid to the validity of the linearity assumptions adopted for the imaging processes (referred to under 'Interpretation of Sample Image') and also that of the fragment removal algorithm.

13 Conclusions

The use of thin membranes supported by fine wire meshes has been shown to provide an effective means of gas separation in Richtmyer-Meshkov instability experiments. Such combinations:

- guarantee fragmentation of membranes;
- enable a range of interface profiles to be used;
- provide good agreement with 3D simulation if an initial small amplitude perturbation of the order of the mesh spacing is used.

14 Future Work

Quantitative analysis is planned using densitometry techniques.

A new shock tube has been ordered (200×100mm), providing operation at higher Mach number and with reduced wall effects.

Additional interface perturbations are to be studied for comparison with 2D turbulence models (including the stepped plane interface study as described by Tolshmyakov at this workshop).

Development of convergent geometry systems.